

Further Insights into the Structure of $[M(\eta^2(C,C)-C_3O_2)(PPh_3)_2]$ ($M = Ni, Pd, Pt$) by Quasi-Relativistic Density Functional Calculations and Solid-State CP/MAS NMR

Maurizio Casarin,^{*,†} Luciano Pandolfo,[‡] and Alessandro Sassi[§]

Dipartimento di Chimica Inorganica, Metallorganica ed Analitica, Università di Padova, Via Loredan, 4, I-35131 Padova, Italy, Dipartimento di Chimica, Università della Basilicata, Via N. Sauro, 85, I-85100 Potenza, Italy, and Dipartimento dei Processi Chimici di Ingegneria, Università di Padova, Via Marzolo, 9, I-35131 Padova, Italy

Received January 16, 2002

The molecular and electronic structures of $[M(\eta^2(C,C)-C_3O_2)(PPh_3)_2]$ ($M = Ni, Pd, Pt$) have been investigated by means of quasi-relativistic gradient-corrected density functional calculations and solid-state CP/MAS NMR spectroscopy. Theoretical outcomes are consistent with a square-planar coordination around the central metal atom and are in very good agreement with the bonding scheme emerging from IR and NMR data.

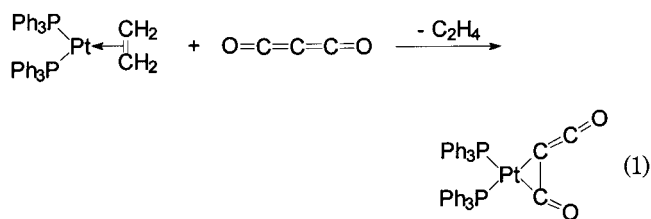
Introduction

For a large number of solids it can be hard to obtain reliable structural information, as they are insoluble in most solvents or change their structures with dissolution. In even worse cases, dissolution may cause decomposition, thus preventing routinely spectroscopic measurements. Even if first-principle quantum-mechanical calculations are not yet considered as a classical analytical tool, it is now widely accepted that the chemical and structural information they provide is often more accessible and likewise reliable than that obtained by conventional methods, thus making first-principle calculations a sort of *new spectroscopy*.¹ In this regard, we recently employed density functional (DF) calculations combined with spectroscopic measurements to get information about the molecular and electronic structure of discrete molecules that are relatively unstable or insoluble.²

Valuable information about solid compounds can be also obtained by solid-state CP/MAS NMR spectroscopy,³ and we have recently used it to look into the structural properties of $Ph_3PC=C=O$ and some related Pt–ketene derivatives.⁴

In this study we have coupled these two techniques to obtain a thorough description of the electronic and

molecular structure of two compounds that cannot be examined in solution. Particularly, about 20 years ago⁵ a compound stable in the solid state but decomposing in solution was synthesized by treating an ethyl ether suspension of $[Pt(\eta^2-C_2H_4)(PPh_3)_2]$ with the bis-ketene carbon suboxide, C_3O_2 (eq 1). Due to its rapid decom-



position in any solvent, the structure of this compound, i.e. $[Pt(\eta^2(C,C)-C_3O_2)(PPh_3)_2]$, was inferred mainly on the basis of elemental analysis and its Nujol IR spectrum.^{5a} This complex was observed to react with I_2 to give C_3O_2 , while with NaOH, sodium malonate is obtained. Comparable results were achieved in the reactions with amines and alcohols that gave malonyl amides and esters, respectively.^{5b} This evidence suggests that C_3O_2 is only weakly bonded to Pt.

Ten years later, the Hillhouse group⁶ synthesized the parent compound $[Ni(\eta^2(C,C)-C_3O_2)(PPh_3)_2]$, characterized by the same instability in solution; besides the Nujol IR spectrum, the solid-state CP/MAS ³¹P NMR data were obtained. Moreover, thanks to the use of ¹³C-enriched C_3O_2 in the synthesis, the authors also recorded the CP/MAS ¹³C NMR spectrum. Spectroscopic data agreed with the structure proposed for the Pt derivative.⁵

We present here the results of a series of quasi-relativistic DF calculations performed on the η^1 -ketenyl-

[†] Dipartimento di Chimica Inorganica, Metallorganica ed Analitica, Università di Padova. Tel: ++39-049-8275164. Fax: ++39-049-8275161. E-mail: casarin@chin.unipd.it.

[‡] Università della Basilicata.

[§] Dipartimento dei Processi Chimici di Ingegneria, Università di Padova.

(1) (a) Ziegler, T. *Chem. Rev.* **1991**, *91*, 651. (b) Parrinello, M. *Solid State Commun.* **1997**, *102*, 107.

(2) (a) Bertani, R.; Casarin, M.; Ganis, P.; Maccato, C.; Pandolfo, L.; Venzo, A.; Vittadini, A.; Zanotto, L. *Organometallics* **2000**, *19*, 1373. (b) Casarin, M.; Pandolfo, L.; Vittadini, A. *Organometallics* **2001**, *20*, 754.

(3) (a) Fitzgerald, J. J., Ed. *Solid State NMR Spectroscopy of Inorganic Materials*, ACS Symposium Series 717; American Chemical Society: Washington, DC, 1999. (b) Bovey, F. A.; Mirau, P. A. *NMR of Polymers*; Academic Press: New York, 1996. (c) Schager, F.; Haack, K. J.; Mynott, R.; Ruffińska, A.; Pörschke, K. R. *Organometallics* **1998**, *17*, 807.

(4) Pandolfo, L.; Sassi, A.; Zanotto, L. *Inorg. Chem. Commun.* **2001**, *4*, 145.

(5) (a) Paiaro, G.; Pandolfo, L. *Angew. Chem., Int. Ed. Engl.* **1981**, *20*, 288. (b) Pandolfo, L.; Morandini, F.; Paiaro, G. *Gazz. Chim. Ital.* **1985**, *115*, 711.

(6) List, A. K.; Smith, M. R., III; Hillhouse, G. L. *Organometallics* **1991**, *10*, 361.

η^2 -ketene⁷ derivatives $[M(\eta^2(C,C)-C_3O_2)(PPh_3)_2]$ (**1**: M = Ni (**a**), Pd (**b**), Pt (**c**)),⁸ combined with solid-state CP/MAS ¹³C and ³¹P NMR spectroscopic data for **1c**.

Experimental Section

General Comments. All reactions and manipulations were carried out under an atmosphere of dry argon with standard Schlenk techniques. Solvents were dried by conventional methods and distilled under argon before use. $[Pt(\eta^2-C_2H_4)(PPh_3)_2]$ ⁹ and C_3O_2 ¹⁰ were synthesized according to the reported methods. IR spectra were taken on a Perkin-Elmer 983 spectrophotometer. Elemental analyses were provided by the Microanalysis Laboratory of the Inorganic Chemistry Department of the University of Padova.

Synthesis of $[Pt(\eta^2(C,C)-C_3O_2)(PPh_3)_2]$. The complex was prepared by slightly modifying the previously reported procedure^{5b} to increase the yield. Complete details of the synthesis and characterization are reported in the Supporting Information.

Solid State CP/MAS NMR Measurements. CP/MAS NMR analyses were performed on a Bruker 200AC spectrometer equipped for solid-state analysis. Details are reported in the Supporting Information.

Computational Details. Actual calculations have been performed on **2a–c** by running the ADF package¹¹ based on DF theory and developed by Baerends and co-workers.¹² Details about the adopted basis sets are reported in the Supporting Information. Nonlocal corrections to the exchange-correlation functional were self-consistently included through the Becke–Perdew¹³ formula. Moreover, all the numerical experiments have been performed at a quasi-relativistic (QR) level.¹⁴ Finally, the metal–ligand binding energies (BE's) have been analyzed by means of the extended transition state method,¹⁵ by considering, as interacting fragments, $(PH_3)_2M$ and C_3O_2 (further details are reported in the Supporting Information). Finally, crystal orbital overlap population (COOP)¹⁶ curves have been computed to get information about the localization and the bonding/antibonding character of selected MO's.

Results and Discussion

Relevant IR features of **1c**^{5a} are reported in Table 1 together with corresponding solid-state ¹³C and ³¹P CP/MAS NMR results.¹⁷ In the same table spectroscopic data pertaining to **1a**⁶ and C_3O_2 ^{18,19} are also included for comparison.

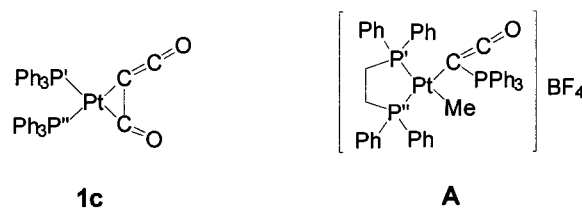
Ketenes can interact with metal systems through C=C and C=O double bonds or O lone pairs, yielding a

Table 1. IR and NMR Data for $[M(\eta^2(C,C)-C_3O_2)(PPh_3)_2]$ (M = Pt, Ni) and Free C_3O_2

M	IR (cm ⁻¹)		³¹ P NMR δ (ppm), J (Hz)	¹³ C NMR δ (ppm), J (Hz)
	ν_{CCO}	ν_{CO}		
Ni ^a	2086	1773	24.8 s 43.6 s	NiC=C=O -12.3 d (² J _{CP} = 16) NiC=C=O 157.7 s NiC=O 187.8 d C ₆ H ₅ 130–138
Pt	2078	1767	P' 28.8 s, ¹ J _{PtP} = 2370 P'' 33.5 s, ¹ J _{PtP} = 4950	PtC=C=O -16.2 d (² J _{CP} = 80) PtC=C=O 151.5 s PtC=O 179.7 d C ₆ H ₅ 129–135
C_3O_2	2280 ^b			C=C=O -14.6 ^c C=C=O 129.7 ^c

^a Reference 6. ^b Reference 18. ^c Reference 19.

Chart 1



large number of different compounds.⁷ Strong signals around 2080 and 1770 cm⁻¹, attributed to the C=C=O and C=O stretching, respectively, indicate for both **1a** and **1c** that only one olefinic (C=C) bond of carbon suboxide is involved in the coordination to the $(PPh_3)_2M$ moiety. Also, ³¹P NMR data for **1a,c** are consistent with the coexistence of η^1 -ketenyl and $\eta^2(C,C)$ -ketene coordination, thus suggesting that C_3O_2 bonds to the metal atom with two distinct M–C bonds. The assignments of ³¹P NMR chemical shifts of **1c** have been carried out by referring to P–Pt coupling constants (¹J_{PtP}) found in complex **A** (Chart 1). Actually, the **A** phosphorus atom trans to the C=C=O moiety (P'') has a ¹J_{PtP} value of ~3500 Hz, while ¹J_{PtP} for P' is definitely lower (~1600 Hz).²⁰ Consistently, we tentatively assign ³¹P NMR chemical shift values of 28.8 and 33.5 ppm to the P' and P'' atoms of **1c**, respectively (see Table 1 and Chart 1).

Analogously to **1a**, the coordinated C_3O_2 gives rise to three different signals in the ¹³C NMR spectrum of **1c**. The two low-field resonances (see Table 1) are indicative of an asymmetric arrangement of the ligand to Pt (δ values of PtC=C=O and PtC=O are in the range previously observed for **1a**⁶). As far as the ¹³C chemical shift of the central carbon atom is concerned, a value very close to that of the free molecule is measured. Analogously to **1a**,⁶ this is indicative of a slight perturbation upon coordination.

To gain further insights into the M– C_3O_2 bonding scheme as well as into the coordination mechanism, we performed a series of QR-DF calculations on the model compounds $[M(\eta^2(C,C)-C_3O_2)(PH_3)]$ (**2**: M = Ni (**a**), Pd (**b**), Pt (**c**)).⁸

Now, before moving to the results of calculations on **2a–c**, we wish to provide a qualitative description of the $(PH_3)_2M-C_3O_2$ bonding scheme mainly based on symmetry arguments and overlap considerations. The

(20) Bertani, R.; Pandolfo, L.; Zanotto, L. *Inorg. Chim. Acta* **2002**, 330, 213.

(7) For the nomenclature of metal complexes involving the CCO moiety see: Geoffroy, G. L.; Bassner, S. L. *Adv. Organomet. Chem.* **1988**, 28, 1.

(8) Theoretical calculations have been performed on model compounds (**2a–c**) where Ph fragments were modeled by H atoms.

(9) Cook, C. D.; Jauhal, G. S. *J. Am. Chem. Soc.* **1968**, 90, 1464.

(10) Klemenc, A.; Wechsberg, R.; Wagner, G. *Monatsh. Chem.* **1935**, 66, 337.

(11) ADF 2000.01; Department of Theoretical Chemistry, Vrije Universiteit, Amsterdam, 2000.

(12) (a) Post, D.; Baerends, E. J. *J. Chem. Phys.* **1983**, 78, 5663. (b) Baerends, E. J.; Ellis, D. E.; Ros, P. *Chem. Phys.* **1973**, 2, 41.

(13) (a) Becke, A. *Phys. Rev. A* **1988**, 38, 3098. (b) Perdew, J. P. *Phys. Rev. B* **1986**, 33, 8822. (c) Perdew, J. P. *Phys. Rev. B* **1986**, 34, 7406.

(14) Ziegler, T.; Tschinke, V.; Baerends, E. J.; Snijders, J. G.; Ravenek, W. *J. Phys. Chem.* **1989**, 93, 3050.

(15) Ziegler, T.; Rauk, A. *Theor. Chim. Acta* **1977**, 46, 1.

(16) Hoffmann, R. *Solids and Surfaces: A Chemist's View of Bonding in Extended Structures*; VCH: New York, 1988.

(17) We tried to synthesize the analogous Pd compound (**1b**), but our attempts were unsuccessful.

(18) Lolck, J. E.; Brodersen, S. *J. Mol. Spectrosc.* **1979**, 75, 234.

(19) Williams, E. A.; Cargioli, J. D.; Ewo, A. *J. Chem. Soc., Chem Commun.* **1975**, 366.

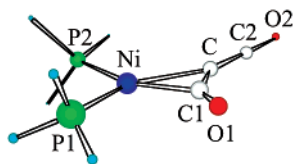


Figure 1. Schematic representation of the optimized structure of **2a**. The structures of **2b** and **2c** are very similar to that of **2a** and have been deposited as Supporting Information.

Table 2. BE's (kcal/mol) of [M(PH₃)₂(C₃O₂)] (M = Ni, Pd, Pt) Model Compounds Decomposed Following Ziegler's Transition-State Analysis

	2a	2b	2c
ΔE_{prep}	24	19	29
ΔE_{ster}	56	55	77
ΔE_{int}	-128	-105	-152
BE	-48	-31	-46

valence manifold of C₃O₂ is characterized by the presence of six molecular orbitals (MO's).^{21,22} In the linear molecule, four of them have π symmetry ($1\pi_u$, $1\pi_g$, $2\pi_u$, and $2\pi_g$)²³ while the remaining two have σ character (σ_g and σ_u). As far as the occupied π set is concerned ($1\pi_u$, $1\pi_g$, and $2\pi_u$), the $1\pi_u$ orbital is totally bonding and quite uniformly distributed over the molecule, the $1\pi_g$ orbital has a node on the central carbon, is C–O bonding, and is more concentrated on the O atoms, and the $2\pi_u$ orbital (the HOMO) is C–C bonding (C–O antibonding) and is highly concentrated on the central carbon and O atoms. The σ_g and σ_u orbitals account for the in-phase and out-of-phase linear combinations of the O lone pairs, respectively. Finally, the $2\pi_g$ LUMO is C–O antibonding and is highly localized on the periph-

Table 3. Selected Structural Parameters for [M(PH₃)₂(η^2 -C₃O₂)] (M = Ni, Pd, Pt) Model Compounds^a

	2a	2b	2c	C ₃ O ₂
BL (Å)				
M–P1	2.136	2.296	2.245	
M–P2	2.222	2.379	2.342	
M–C	1.910	2.104	2.073	
M–C1	1.892	2.083	2.059	
C1–O1	1.207	1.202	1.204	1.172
C–C1	1.373	1.359	1.396	1.274
C–C2	1.288	1.287	1.290	1.274
C2–O2	1.181	1.181	1.180	1.172
BA (deg)				
P1–M–P2	112.0	110.9	106.3	
C–M–C1	42.3	37.9	39.5	
O1–C1–M	141.6	135.8	142.8	
C2–C–M	141.2	140.6	141.9	
C1–C–C2	150.3	149.0	146.8	175.8
O1–C1–C	148.9	152.3	146.4	179.5
O2–C2–C	176.5	175.5	176.9	179.5
P1–M–C1–O1	0.3	0.3	-0.5	
P1–M–C–C1	0.9	0.3	-1.7	

^a Structural parameters computed for the free C₃O₂²² are also included for comparison. Refer to Figure 1 for the atom labeling.

eral C atoms. Among these MO's, those of greatest interest with respect to the C₃O₂ molecular reactivity²⁴ are the $2\pi_u$ HOMO and the $2\pi_g$ LUMO, accounting for the C₃O₂ donor and acceptor properties, respectively. According to the bonding/antibonding characteristics of the C₃O₂ frontier MO's, and within the assumption of similar MO shapes for the free and coordinated ligand, the C₃O₂→M donation should imply a lengthening (shortening) of the C–C (C–O) bond length (BL), while the M→C₃O₂ back-donation should scarcely affect the C–C BL and eventually stretch out the C–O bond.

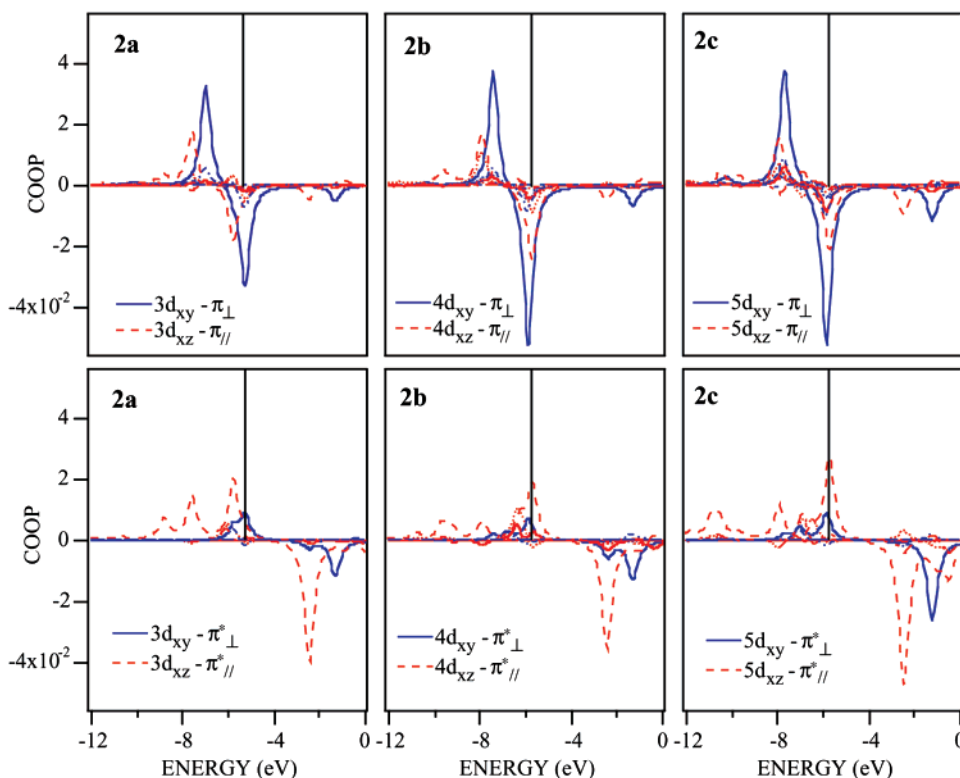


Figure 2. COOP between the M *nd* and C₃O₂ $2\pi_u$ HOMO (top) and the M *nd* and C₃O₂ $2\pi_g$ LUMO (bottom). Both parallel (\parallel) and perpendicular (\perp) contributions have been considered. Bonding and antibonding states correspond to COOP positive and negative peaks, respectively. Vertical bars represent the HOMO energy.

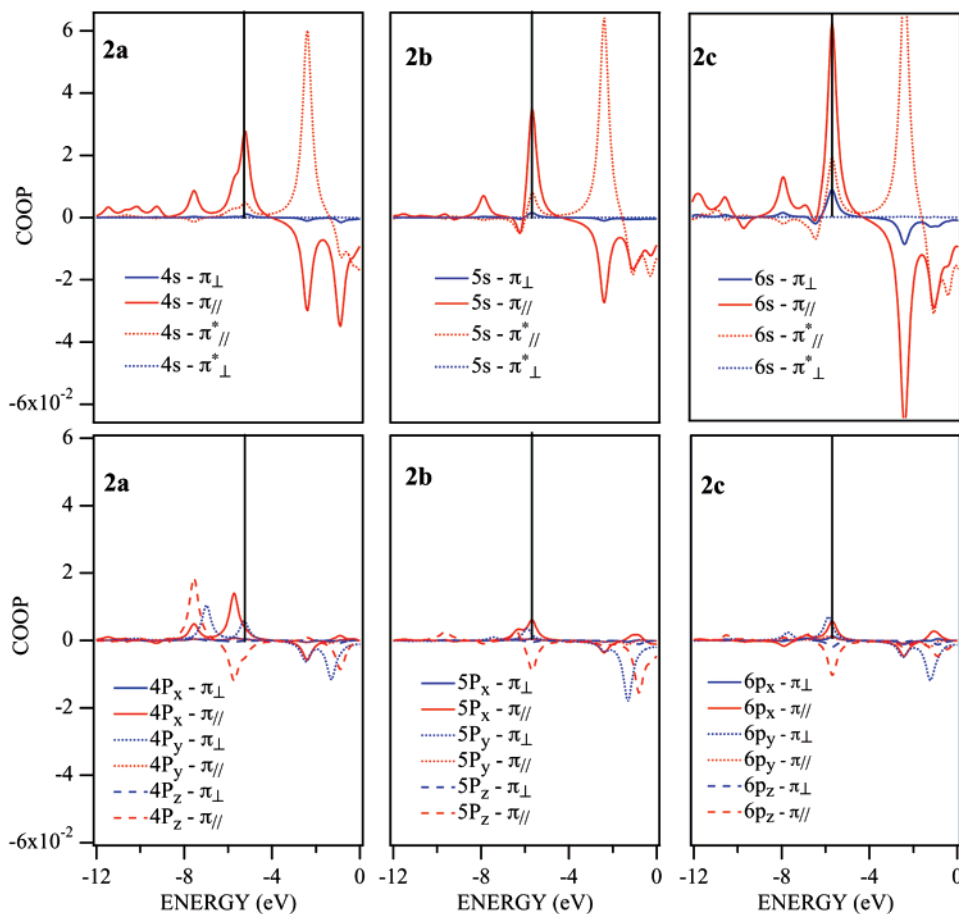


Figure 3. COOP between the M ($n + 1$)s/p and C_3O_2 $2\pi_u$ HOMO (top) and the M nd and C_3O_2 $2\pi_g$ LUMO (bottom).

Two other things have to be considered before addressing the analysis of the results of QR-DF calculations: (i) $d^{10} ML_2$ moieties form adducts with unsaturated species, such as olefins, which result in side-on coordination to the metal;²⁵ (ii) as a consequence of the topology of the $d^{10} ML_2$ fragment MOs, the *in-plane* coordination of the unsaturated molecule is the most favorable arrangement.^{26–28}

As a whole, all these issues allow us to foresee that (i) the interaction between the completely occupied M nd atomic orbitals (AO's) and the C_3O_2 $2\pi_u$ HOMO should have an overall destabilizing effect and (ii) the M– C_3O_2 bonding should be characterized by two contributions, one involving donation from the C_3O_2 $2\pi_u$

HOMO into M ($n + 1$)s/p AO's, the other implying back-donation from M nd AO's into the C_3O_2 $2\pi_g$ LUMO.

In Tables 2 and 3 BE's decomposed according to Ziegler's transition-state analysis¹⁵ and selected structural parameters of **2a–c** are reported, respectively. Optimized BL's and BA's computed for the free C_3O_2 ²² have been also included in Table 3 for comparison. Data from Table 2 indicate very similar BE's for **2a,c**, while, in agreement with our failure to synthesize **1b**, the $(PH_3)_2Pd-C_3O_2$ bonding is definitely weaker. As far as the optimized geometrical parameters included in Table 3 are concerned, they point out that, along the whole series, (i) the molecular geometry of C_3O_2 is perturbed to a significant and similar extent upon coordination (see Figure 1) and (ii) according to the qualitative discussion reported above, both C–C1 and C1–O1 BL's are lengthened upon coordination (the former much more than the latter). Further insights into the $(PH_3)_2M-C_3O_2$ bonding scheme can be gained by referring to Figures 2 and 3, where COOP's between M AO's and C_3O_2 frontier orbitals are displayed. The inspection of Figure 2 testifies that, as foreseen, the only bonding interaction involving the M nd AO's (in particular nd_{xz} and nd_{xy} in the adopted framework) is that of back-bonding into the MO's reminiscent of the doubly degenerate C_3O_2 $2\pi_g$ LUMO (hereafter, $\pi^*_{||}$ and π^*_{\perp}). Interestingly, back-donation seems more efficient in **2a,c** than in **2b**. For the COOP's reported in Figure 3, the presence of a quite strong donation of the C_3O_2 HOMO into the Ni 4p AO's and Pt 6s AO is well evident. It is

(21) Connolly, J. W. D.; Seibahn, H.; Gelius, U.; Nordling, C. *J. Chem. Phys.* **1973**, *58*, 4265.

(22) Some of us are revisiting the electronic structure of the free C_3O_2 by coupling extended basis set DF calculations to variable-energy photoelectron spectroscopy. The corresponding manuscript is in preparation.

(23) Throughout the paper the C_3O_2 π and σ orbitals have been labeled according to the irreducible representations of the D_{3h} symmetry point group: i.e., by assuming a linear geometry for the free molecule.

(24) Miessler, G. L.; Tarr, D. A. *Inorganic Chemistry*, 2nd ed.; Prentice-Hall: Englewood Cliffs, NJ, 1998.

(25) (a) Hartley, F. R. *Angew. Chem.* **1972**, *84*, 657. (b) Vaska, L. *Acc. Chem. Res.* **1976**, *9*, 175.

(26) Ziegler, T. *Inorg. Chem.* **1985**, *24*, 1547.

(27) In the adopted framework the coordination plane corresponds to the xz plane.

(28) A further series of numerical experiments has been carried out for **2a–c** within the assumption of an *out-of-plane* coordination of C_3O_2 . As expected, corresponding BE's resulted always significantly lower than those for the *in-plane* configuration.

also manifest that Pd 5p AO's interact with the C₃O₂ HOMO to a negligible extent, while the Pd 5s AO does not seem to exceed the involvement of the Ni 4s AO in its interaction with the $\pi_{||}$ component of the C₃O₂ HOMO.

The M–C₃O₂ bonding picture emerging from all these data is consistent with quite similar interactions of Ni and Pt with C₃O₂. In both cases there is a comparable M→C₃O₂ back-donation from $nd_{xy/xz}$ into C₃O₂ $\pi^*_{||}/\pi^*_{\perp}$ orbitals, assisted by a C₃O₂→M donation (negligible in **2b**) involving either Ni 4p AO's or the Pt 6s AO (as a consequence of relativistic effects²⁹). According to this, the Hirshfeld charges³¹ of the coordinated C₃O₂ fragment are quite similar along the series (–0.29, –0.32, and –0.29 in **2a–c**, respectively), consistent with a net charge transfer from the (PH₃)₂M moiety to the C₃O₂ ligand. Even if this is compatible with a C₃O₂ oxidative addition, the lower ΔE_{int} value of the Pd derivative stresses that, besides back-donation, an important role is played by C₃O₂→M donation to stabilize the complexes.

Vibrational parameters pertinent to **2a** and **2c** have been computed. Theoretical values of $\nu_{\text{CCO}}/\nu_{\text{CO}}$ are 2169/

(29) The mass increase of s electrons with high instantaneous velocities near the nucleus has the effect of contracting and stabilizing the s orbitals, thus destabilizing the 5d levels, whose electrons experience a reduced effective nuclear charge.³⁰

(30) Pyykkö, P.; Declaux, J.-P. *Acc. Chem. Res.* **1979**, *12*, 276.

(31) (a) Hirshfeld, F. L. *Theor. Chim. Acta* **1977**, *44*, 129. (b) Wiberg, K. B.; Rablen, P. R. *J. Comput. Chem.* **1993**, *14*, 1504.

1855 cm^{–1} (**2a**) and 2152/1833 cm^{–1} (**2c**), while the ν_{CCO} frequency computed for free C₃O₂ is 2364 cm^{–1}. The comparison with IR data reported in Table 1 indicate an absolute overestimation of ~60/80 cm^{–1}; nevertheless, according to the proposed bonding scheme, ν_{CCO} undergoes a significant red shift upon coordination (204 and 212 cm^{–1} in **1a,c**, respectively), which is quantitatively reproduced by QR-DF calculations (195 and 212 cm^{–1} in **2a,c**, respectively).

Conclusions

In this contribution we have presented the results of an experimental and theoretical study concerning the electronic and molecular structure of a series of complexes highly unstable in solution. As far as the M–C₃O₂ coordination is concerned, QR-DF calculations agree with IR and CP/MAS NMR data in predicting two distinct M–C bonds. Moreover, theoretical results also indicate a significantly higher stability of Ni and Pt complexes compared to [Pd(η^2 (C,C)-C₃O₂)(PPh₃)₂]. This has been ultimately ascribed to a stronger C₃O₂→M donation in Ni and Pt derivatives which involves the 4p AO's in **2a** and the 6s AO, stabilized by relativistic effects, in **2c**.

Supporting Information Available: This material is available free of charge via the Internet at <http://pubs.acs.org>.

OM0200353